Mechanical strength of nanocrystalline/amorphous $Al_{90}Fe_5Gd_5$ composites produced by rolling

W. H. Jiang
Department of Nuclear Engineering and Radiological Sciences, University of Michigan, Ann Arbor, Michigan 48109

M. Atzmon[a)]
Department of Nuclear Engineering and Radiological Sciences and Department of Materials Science and Engineering, University of Michigan, Ann Arbor, Michigan 48109

(Received 24 November 2004; accepted 1 March 2005; published online 7 April 2005)

Mechanical deformation is expected to be an alternative route for synthesizing nanocrystalline/amorphous matrix composites. However, it is found that nanocrystalline/amorphous $Al_{90}Fe_5Gd_5$ composites produced by cold rolling have lower hardness than the as-spun, fully amorphous, alloy. Much smaller pileups are observed around indents in rolled samples than in the as-spun sample. Combining high-resolution transmission electron microscopy with Fourier transform and image filtering, many nanovoids are observed in the shear bands near the boundary with the undeformed matrix. © *2005 American Institute of Physics*. [DOI: 10.1063/1.1897434]

Reinforcements/amorphous matrix composites have received much attention in recent years. Among them, nanocrystalline/amorphous matrix composites exhibit excellent mechanical properties.[1–6] Such composites are typically formed by partial crystallization of the amorphous phase at elevated temperatures or melt quenching at reduced rates.[5–7] Hardening has been attributed to a direct effect of the nanocrystals[1] or to solute enrichment of the remaining amorphous matrix.[5] It has been found that mechanical deformation, such as bending,[8,9] high-energy ball milling,[10] tension,[11] as well as nanoindentation,[12,13] can also induce nanocrystallization in amorphous alloys. One would expect this process to be an alternative route of synthesizing nanocrystalline/amorphous matrix composites.[8,10,13] While many studies have addressed the effect of plastic deformation on the microstructural evolution of amorphous alloys, very little attention has been given to the resulting effect on mechanical properties.

In the present work, the effect of cold rolling on the hardness of an amorphous $Al_{90}Fe_5Gd_5$ alloy, obtained by single-wheel melt-spinning,[9] is investigated and correlated with the change in microstructure. X-ray and electron diffraction analyses were employed to confirm the amorphous structure of the as-spun alloy ribbon (22 μm thick and 1 mm wide). Samples were rolled in up to 100 small steps to final thickness reductions of 22.7% and 45.5%, respectively. Samples were prepared for nanoindentation and transmission electron microscopy (TEM) by polishing from the wheel side, using a single-jet electropolisher.[12] Instrumented indentation was performed with a diamond Berkovich indenter, under load control, at a rate of 0.5 mN/s.[12] The hardness values were corrected for the effect of pileups by determining the actual contact area, using atomic force microscopy (AFM).

TEM observation shows that numerous, curved, shear bands, formed after rolling, indicating inhomogeneous plastic deformation [Fig. 1(a)]. In a selected-area electron diffraction (SAED) pattern [Fig. 1(b) inset], diffuse rings originating from the amorphous matrix, plus four sharp diffraction rings, are observed, indicating the occurrence of crystallization. A dark-field image [Fig. 1(b)] reveals nanocrystallites at a shear band. The TEM sample preparation process and electron beam have been ruled out as causes of crystallization.[9] These results demonstrate that rolling at room temperature induced nanocrystallization. However, unlike for nanocrystallites induced by a thermal route, which are evenly distributed, the nanocrystals produced by mechanical deformation are unevenly distributed since they are confined to shear bands.

Figure 2 shows the hardness of the as-spun and rolled samples at various depths, as derived from nanoindentation.

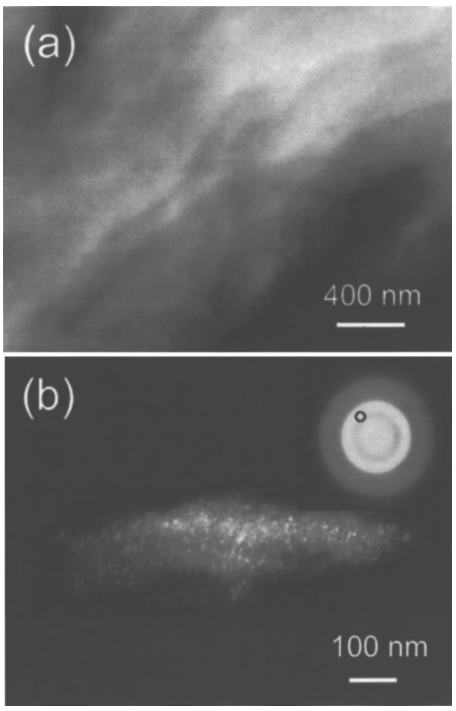

FIG. 1. TEM images of a sample rolled with thickness reduction of 45.5%, (a) bright-field and (b) dark-field images with its SAED pattern (inset) where the position of the objective aperture is illustrated.

[a)]Electronic mail: atzmon@umich.edu

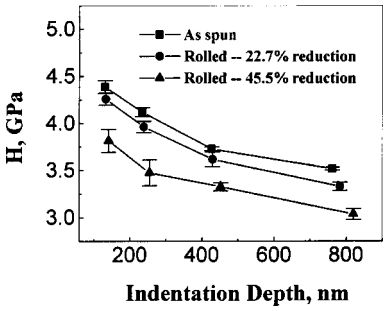

FIG. 2. Hardness values obtained from nanoindentation tests at various indentation depths.

For all samples, the hardness decreases with increasing depths. At the micro/nanometer scale, depth-dependent hardness has been observed in both crystalline and amorphous materials.[14–18] It has been explained by strain-gradient plasticity[19,20] in the former and a surface contribution in the latter.[21] Wright and Nix[18] attributed this size effect in a metallic glass to decreasing probability of finding a large density fluctuation with decreasing indentation depth. Surprisingly, the rolled samples, containing deformation-induced nanocrystallites, have lower hardness than the as-spun, fully amorphous, sample. The hardness decreases with increasing thickness reduction.

AFM observation in the as-spun and rolled samples indicates that the indents were rather regular in shape and caused no cracking. Typical images and their corresponding height profiles are shown in Fig. 3. There are very obvious pileups around the indents in the as-spun sample, with height of about 44% of the indent depth, while in the rolled sample the height of the pileups is only 14% of the indent depth.

Figure 4(a) is a high-resolution TEM (HRTEM) image containing both a part of shear band and its neighboring, undeformed, matrix. Nanocrystalline particles are observed in the interior of the shear band. Following Miller and Gibson[22] and Li *et al.*,[23] we imaged the region of Fig. 4(a) at a defocus value of −200 nm.[9] In order to image defects giving rise to the small-angle scattering, the Fourier transform was subjected to an annular filter that passed the spatial frequencies of interest ($0.5\ \text{nm}^{-1} < k < 1.5\ \text{nm}^{-1}$) and excluded all other spatial frequencies. A reverse Fourier transform was

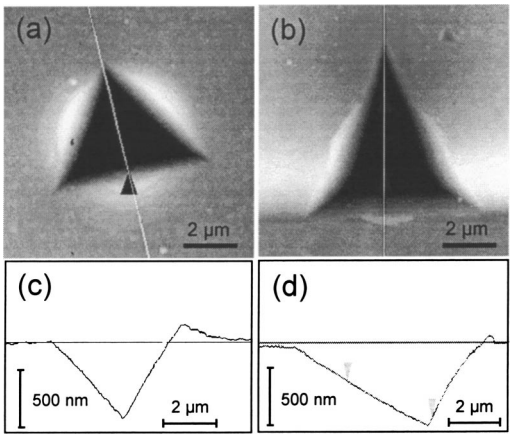

FIG. 3. (a) and (b) AFM images, (c) and (d) height profiles along the lines indicated in (a) and (b), respectively. The indents were formed at the maximum load of 50 mN in the as-spun sample [(a) and (c)], and in the rolled sample with thickness reduction of 45.5% [(b) and (d)].

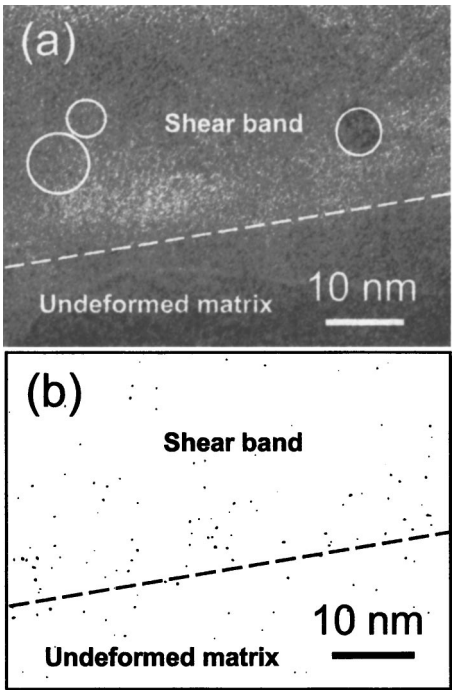

FIG. 4. (a) HRTEM image showing a part of a shear band and its neighboring, undeformed, matrix in the sample rolled with thickness reduction of 45.5%, (b) image at the same position as (a), but defocused −200 nm, Fourier filtered, threshold filtered, and inverted. The lines indicate the boundary between the shear band and undeformed region.

computed to obtain a filtered image, which displays the projected atomic density. It does not contain contributions from the sample's thickness variations, since these have long wavelength, hence, the uniform average intensity. To identify defects in the alloy, a threshold filter was then applied, set to pass a signal only when the mean brightness is exceeded by three standard deviations. Black and white were then inverted for greater clarity. The resulting image is shown in Fig. 4(b), with the small spots indicating the location of low-density defects in Fig. 4(a). We will refer to these defects as nanovoids.[22,23] They are concentrated in the shear band, mainly near the boundary with the undeformed matrix. The interior of the shear band has few nanovoids, as does the undeformed region, in agreement with our observation on the compressive region in the same alloy ribbon bent at room temperature.[9] Li *et al.*[23] observed a higher density of nanovoids in shear bands at the tip of cracks developed during sample preparation by electropolishing.

Donovan and Stobbs,[24] in their model of shear bands, argued that a shear band is dilated even when under compression. A large proportion of the atoms within shear bands are subject to local displacements. Thus, atomic dilatation in the shear bands is the likely cause of enhanced atomic mobility and, hence, it assists crystallization. When shear bands form under tensile stress, they contain a uniform distribution of nanovoids, likely a result of coalescence of free volume.[9] As a crystalline solid is denser than its amorphous counterpart, crystallization within shear bands may also result in the formation of nanovoids.

Deformation softening has been observed in amorphous alloys.[25] However, the authors are not aware of previous reports on the effect of nanocrystallization. Undoubtedly, the decrease in strength is due to the formation of shear bands during the deformation process, which are weaker regions in

amorphous alloys. Despite the fact that nanocrystallites can often strengthen the amorphous matrix, as in nanocrystalline/amorphous matrix composites produced by thermal route,[1,26,27] the nanocrystallites in shear bands produced during deformation fail to compensate for deformation softening resulting from the shear bands themselves. The AFM results demonstrate that, compared with the as-spun sample, the rolled samples have much smaller pileups around indents. In the as-spun sample, obvious pileups around indents indicate that during nanoindentation, inhomogeneous deformation occurred, and its mechanism is one of nucleation and propagation of new shear bands. In the rolled sample, the small height of pileups around the indents indicates that few new shear bands were generated during nanoindentation, and the predominant deformation mechanism is the propagation of pre-existing shear bands, developed during rolling, beneath indents. Pileups on the surface around indents were found to be only a small part of the total deformation.[28] Again, this demonstrates that preexisting shear bands in the rolled sample are weaker regions, even though they contain nanocrystallites. HRTEM observation reveals the formation of the numerous nanovoids in the shear bands, along the boundaries with the undeformed matrix, after rolling [Fig. 4(b)]. The formation of larger voids at shear bands was observed in a bulk Pd-based amorphous alloy deformed about 40%.[29] Work is underway to determine whether the nanovoids we observed affect the strength.

In summary, the nanocrystalline/amorphous matrix composites produced by cold rolling have lower mechanical strength than the as-spun, fully amorphous, alloy. Nanovoids formed during rolling are concentrated in the shear bands near the boundary with the undeformed matrix. The formation of defects may be important when nanocrystallization in amorphous alloys is pursued by the route of mechanical deformation.

The authors are grateful to Dr. F. E. Pinkerton (General Motors Research Laboratories) for providing the samples used in this study. The electron microscopy, AFM, and nanoindentation work was performed at the Electron Microbeam Analysis Laboratory at the University of Michigan, Ann Arbor, MI. This work was funded by the U.S. National Science Foundation, Grant No. DMR-0314214.

[1] Y. H. Kim, A. Inoue, and T. Masumoto, Mater. Trans., JIM **32**, 331 (1991).
[2] L. Q. Xing, J. Eckert, and L. Schultz, Nanostruct. Mater. **12**, 503 (1999).
[3] L. Q. Xing, C. Bertrand, J. P. Dallas, and M. Cornet, Mater. Sci. Eng., A **241**, 216 (1998).
[4] H. Chen, Y. He, G. J. Shiflet, and S. J. Poon, Scr. Metall. Mater. **25**, 1421 (1991).
[5] T. Gloriant and A. L. Greer, Nanostruct. Mater. **10**, 389 (1998).
[6] A. L. Greer, Mater. Sci. Eng., A **304–306**, 68 (2001).
[7] J. Q. Wang, X. C. Chang, W. L. Hou, K. Lu, and Z. Q. Hu, Philos. Mag. Lett. **80**, 349 (2000).
[8] H. Chen, Y. He, G. J. Shiflet, and S. J. Poon, Nature (London) **367**, 541 (1994).
[9] W. H. Jiang and M. Atzmon, Acta Mater. **51**, 4095 (2003).
[10] Y. He, G. J. Shiflet, and S. J. Poon, Acta Metall. Mater. **43**, 83 (1995).
[11] M. C. Gao, R. E. Hackenberg, and G. J. Shiflet, Mater. Trans., JIM **42**, 1741 (2001).
[12] W. H. Jiang, F. E. Pinkerton, and M. Atzmon, J. Appl. Phys. **93**, 9287 (2003).
[13] Y. F. Deng, L. L. He, Q. S. Zhang, H. F. Zhang, and H. Q. Ye, Adv. Eng. Mater. **5**, 738 (2003).
[14] Q. Ma and D. R. Clarke, J. Mater. Res. **10**, 853 (1995).
[15] H. Gao, C. H. Chiu, and J. Lee, Int. J. Solids Struct. **29**, 2471 (1992).
[16] A. C. M. Chong and D. C. C. Lam, J. Mater. Res. **14**, 4103 (1999).
[17] A. Krell and S. Schadlich, Mater. Sci. Eng., A **307**, 172 (2001).
[18] W. J. Wright, R. Saha, and W. D. Nix, Mater. Trans., JIM **42**, 642 (2001).
[19] W. D. Nix and H. Gao, J. Mech. Phys. Solids **46**, 411 (1998).
[20] D. C. C. Lam and A. C. M. Chong, J. Mater. Res. **14**, 3784 (1999).
[21] T. Y. Zhang and W. H. Xu, J. Mater. Res. **17**, 1715 (2002).
[22] P. D. Miller and J. M. Gibson, Ultramicroscopy **74**, 221 (1998).
[23] J. Li, Z. L. Wang, and T. C. Hufnagel, Phys. Rev. B **65**, 144201 (2002).
[24] P. E. Donovan and W. M. Stobbs, Acta Metall. **29**, 1419 (1981).
[25] T. Masumoto and R. Maddin, Mater. Sci. Eng. **19**, 1 (1975).
[26] W. S. Sun and M. X. Quan, Mater. Lett. **27**, 101 (1996).
[27] H. S. Kim, Scr. Mater. **48**, 43 (2003); Mater. Sci. Eng., A **304–306**, 327 (2001).
[28] P. E. Donovan, J. Mater. Sci. **24**, 523 (1989).
[29] C. A. Pampillo and H. S. Chen, Mater. Sci. Eng. **13**, 181 (1974).